

RESEARCH ARTICLE

A Hybrid Macro and Micro Method for Consumer Emotion and Behavior Research

MO XIAOHONG¹, XIE ZHIHAO², AND LUH DING-BANG¹ ¹School of Art and Design, Guangdong University of Technology, Guangzhou 510075, China²School of Electromechanical Engineering, Guangdong University of Technology, Guangzhou 510075, China

Corresponding author: Luh Ding-Bang (ding-banglu@163.com)

This work was supported in part by the Provincial Laboratory Research Association under Grant GDJ20220262, and in part by the 2022 Higher Education Scientific Research Planning Subjects under Grant 22SY0105.

ABSTRACT To investigate impacts of intelligent and fashion factors of sports bras on consumers' emotions, decision-making and behavior, a quantitative analysis method combing macro affective computing and micro emotion data was proposed. The context where a consumer purchased sports bras was first simulated. In this process, an eye tracker and a multi-channel physiological recorder were utilized to collect physiological signal data from participants in an experimental setting. Then, big data and machine learning were both adopted to macroscopically perform data pre-processing, build a computational model, fulfill relevant prediction and evaluation, analyze correlations in physiological data features, and explore potential values existing in data. Furthermore, highly correlated data features were extracted to investigate micro causalities and identify reasons why consumer behavior and decision-making were supported by data about emotional physiology. The proposed method may provide considerably reliable data support for designers, product service providers, and other practitioners. As an innovative and universal integration approach, it has the potential to be applied in medical science, psychology, management science and other fields.

INDEX TERMS Emotion recognition, consumer behavior, machine learning, emotional physiology experiment.


I. INTRODUCTION

A. BACKGROUND AND MOTIVATION

Emotions that arise from consumers when facing specific products and services are their most direct psychological feelings. They are generally deemed as the key evaluation indicators influencing consumers' attitudes, behaviors and decision-making [1]. Therefore, many enterprises select emotion recognition techniques and corresponding data analysis skills to investigate consumers' emotional experience, assist them in better understanding such emotional experience, and provide data support for customer experience improvement [2].

The research on consumers' emotions relates to multiple disciplines of psychology, marketing, and consumer behavior., and different disciplines require different research methodologies, leading to differences in their research

frameworks, sampling deviations, long-term effects and quantification standard differences [3]. To this end, it is necessary to integrate dominant approaches in various disciplines, and raise standardized emotion recognition and data analysis methods of high accuracy and reliability. Chen believed that further study may combine various methods and techniques to enhance research reliability and accuracy [4]. According to multiple literature reviews, it is rather ideal to combine physiological data with machine learning in a macro and micro research framework [5], [6], [7]. On one hand, big data and machine learning that focus on macro affective computing, featuring natural advantages in data value finding and source tracing, are beneficial to identifying the corresponding data law and building a mathematical model accordingly [8]. On the other hand, micro quantitative analysis methods based on emotional physiological experiments can more truthfully reflect consumers' emotions, assist designers and product service providers in comprehending consumers' real emotional responses in the face of products and services, and eventually

The associate editor coordinating the review of this manuscript and approving it for publication was Byung Cheol Song .

identify the causality between consumers' emotion and their purchase decision [9], [10].

By simulating a scenario of consumers purchasing sports bras online, a synesthesia experiment was built by virtue of an eye tracker and a multi-channel physiological recorder to acquire the emotional physiological signals of consumers facing different products and services. Subsequently, macro and micro methods were further adopted to analyze emotional physiological data. In this way, certain support can be provided for product design and marketing strategies formulated by designers and product service providers.

B. RELATIVE RESEARCH

Many methods are available for the investigation of emotions. With advances in cognitive psychology and relevant devices and technologies, emotion self-report, emotion rating scales such as PAD and behavioral analysis and other traditional methods have been gradually substituted by micro emotional physiological experiments or other macro methods of big data and machine learning, as a result of subjectivity and inaccuracy. Micro emotional physiological experiments can reflect the real emotions of human beings and interpret causes and effects of the emotion. Now, it is rather popular in the fields of psychology, education, and management. In terms of macro affective computing, data crawling was fulfilled by virtue of open-source databases or the network, featuring a large data size, the capability of reflecting emotion law, and an ability to explore correlations of emotions to some events. It has made rapid progress in the disciplines of computer science, artificial intelligence, and communications. For the past few years, as a new trend, micro physiological experiments and macro affective computing are becoming increasingly combined [11].

1) MICRO EMOTIONAL PHYSIOLOGICAL EXPERIMENTS

The micro method of emotion studies primarily utilizes and probes into the neuromechanism of emotion generation and relevant data such as physiological signals, which contributes to the understanding of causes and effects of emotion generation. Lang et al. summarized the physiological bases of emotions and corresponding experimental approaches, including definitions of emotion, the relationship of emotion and physiological responses, and the neuromechanism of emotion [12], and also discussed emotional expressions in different areas of the brain (e.g., amygdaloid nucleus, prefrontal cortex, gyrus cinguli, corpus striatum, and hypothalamus), confirming a neural basis for emotions. In addition to analyzing correlations between emotion and the autonomic nervous system (ANS), Kreibig also introduced the effects of two ANS branches (i.e., sympathetic nerve and parasympathetic nerve) on emotions and some methods of measuring ANS activity [13]. These studies have proven that physiological responses are an indicator to measure and learn about emotional responses, and emotions can place certain influences on physiological responses as well.

Most of the existing micro emotion research methods are dependent on nerve and physiological signal changes caused by emotional stimulus materials such as images, sounds, and videos [14]. Considering that different emotional stimulus materials may lead to different physiological responses, such as changes in the mean heart rate (mean HR), heart rate variability (HRV), electrodermal activity, and skin temperature, scholars adopted electroencephalograph, multi-channel physiological recorders, eye trackers and brain imaging devices to collect physiological signals from participants simulated by experimentally simulated events. Through measurements of such physiological indicators, the emotional status of human beings can be inferred [15]. In another literature, it is pointed out that emotional videos can be utilized to estimate the accuracy of recognizing emotional types and sensitivity of emotional intensity, which shows satisfactory reliability and accuracy [16].

In accordance with consumer behavior, micro studies on emotions are mostly targeted at emotions and purchase behavior of consumers, and thus provide evidence for designers and product service providers for product design and marketing strategy formulation. For example, [17] developed a new method based on color-emotion associations. To be specific, an eye tracker was utilized to detect consumers' repressed emotions. Non-invasive physiological data acquisition devices such as eye trackers and multi-channel physiological recorders can rapidly recognize such repressed emotions, which facilitates a better understanding of consumer behavior [18]. Moreover, emotional valence and emotion arousal level, as two emotional attributes, are independent of the influence from other dimensions including sociality; for this reason, they are preferably independent and have been widely applied in studies on consumers' emotions and behaviors [19]. Mauss et al. explored the coordination in emotional experience, behavior, and physiological responses, and the experimental results proved the existence of certain coordination. More particularly, consistency between emotional experience and physiological responses can be adopted to predict behavior [20] and consumers' purchase behavior [21] used a meta-analysis method to investigate two theories of emotion-as-direct-causation and emotion-as-feedback, and both theories believed that emotions have a direct influence on individuals' behavior and decision-making.

The literature mentioned above not only contributes to a more in-depth understanding of the physiological mechanism of emotional responses, but also provides research on relevant fields with some important experimental foundations and data support. Some studies can more objectively reflect the physiological mechanism of emotions and be more persuasive in revealing repressed emotions and the in-depth relationships of events and emotion generation, as they are based on actual physiological emotions of individuals [22] suggested that future studies on emotions should measure the implicit attitude of emotions and its potential associations with the corresponding psychological process.

2) MACRO AFFECTIVE COMPUTING

Macro affective computing consists of three main aspects, physiological data processing, the computing model, and the evaluation method. In general cases, expertise-based historical data contain the acquired physiological data and also independent and dependent variables of the computing model. In the field of medical science, for example, examination data are usually used as independent variables, while diagnosis reports given by a doctor as dependent variables, so as to build a machine learning model. As far as emotion recognition is concerned, facial recognition results of users serve as the dependent variable of emotions. Considering that facial recognition is of significantly high accuracy [23], physiological signals collected from a user are used as the independent variable [24]. In this context, the corresponding machine learning model can be constructed. Additionally, users' preference selection in a questionnaire survey is selected as the dependent variable in many studies, however, this is dramatically subjective. In general, emotion recognition based on machine learning and physiological signals is heatedly discussed for the past few years as it performs better in learning hierarchical features of physiological signals, gives sufficient consideration to contextual information, and has the capability of efficiently expressing complicated patterns implied in data [25].

In terms of physiological data, problems arising during their acquisition, such as noise and interference, make it difficult to directly apply these data to analysis and modeling. Therefore, data should be pre-processed before physiological data analysis and mining to eliminate noise, perform filtering and reduce dimensionality. For example, [24] used Savitzky-Golay smoothing filter to effectively remove noise from input signals, and combined wavelet scattering with wavelet synchrosqueezed transform to transform multi-modal single-dimensional physiological signals into two-dimensional images, to improve feature extraction and classification performance of physiological signals. Three emotions datasets AMIGOS, DREAMER, and SWELL were taken as examples in [26] for resampling of electrocardiogram (ECG) in SWELL dataset, during which high-pass filtering was adopted to eliminate low-frequency signals generated by electrode polarization. Subsequently, z-score normalization was performed for signals of every sensor; and ECG signals were segmented by a 10-second non-overlapping sliding window. After features of physiological signals in DEAP dataset, including dermal resistance, respiratory rates, and HRV, were extracted using Fourier transform and classical statistics, linear discriminant analysis on these features was conducted [27]. In a word, data pre-processing is a mature technique, and there are many sophisticated solutions available for related studies, which can also produce expected effects [28].

Regarding computing models, they are generally concerned with training, testing, and testing result evaluation. Affective computing is mainly classified into one based on

information and one based on physiological information of human beings. For information-based affective computing, it involves online public sentiment based on natural language processing and communication based on social media [29]. In emotions related studies based on images and texts, a three-image two-text classification model were used in [30] to recognize emotions in images and texts, proposing that two emotion prediction methods can be synthesized as an output of the multi-modal emotion recognition model. In this way, not only is the multi-emotional relationship in samples qualitatively and quantitatively described, but emotional confusion and migratory direction of samples are elaborated from the perspective of emotion recognition models, thus providing a theoretical basis and direction for the improvement of model performance by prior knowledge. There also exists affective computing based on robotics [31]. Emotions are also investigated based on physiological information of human beings, such as HRV, an objective measurement of emotion regulation capability indexes [32] revealed that specific difficulties in emotion regulation are associated with low vagus-mediated HRV (vmHRV). Moreover, self-reported emotion regulation difficulties form a negative correlation to resting and 24-hour vmHRV. Through comparative studies on experimental physiological data and seven machine learning approaches for automatic emotion recognition in safe driving, [33] intended to find a method best for developing a personalized adaptive emotion estimator. By extracting features from EEG signals and selecting machine learning for emotion classification, a new interpretable emotion recognition method with an activation mechanism was proposed in [34]. In the experimental process, emotions are gradually activated, and EEG-based emotion recognition accuracy can be effectively boosted by weighting coefficients of correlation and entropy coefficients of emotions [35] proposed an amygdaloid nucleus inspired affective computing framework to recognize various personalized emotions of human beings.

As described above, traditional affective computing research focuses on exploring explicit emotions. For example, recognition of emotional state depends mainly on facial expressions and voices, which fails to sufficiently investigate implicit emotional relationships. Compared with facial expressions and voice features, physiological signals are primarily associated with autonomic nervous system activity. Consequently, voluntary and conscious manipulations over physiological signals can be more difficult than those over facial expressions [36], and recognition accuracy is also comparatively low. However, emotion recognition based on physiological signals still has certain advantages as follows: (1) Emotional state can be continuously monitored, as physiological signal data are continuous; (2) emotion detection is allowed anytime anywhere as physiological sensors are small-sized wearable devices and there are many mature solutions available [37], [38]; and (3) although emotion recognition based on facial expressions and voices is preferably accurate, emotion recognition based on physiological

signals features a dominant effect of describing the causes and consequences of emotions (i.e., stories) [39]. Now, multi-modal data-based emotion recognition attracts increasingly more attention as emotion studies need to focus on real emotional responses of human beings, correlations of emotions to behavior, and the macro law of emotions [40].

II. EXPERIMENTS AND DATA COLLECTION

Eye tracker Eyelink 1000 Plus and multi-channel physiological recorder BIOPAC MP160 were used to perform synesthesia experiments in a standard Stimuli-Organism-Response model, simulating a scenario of online product sales and studying consumers' emotional experience once they catch sight of product pictures. First, pictures of average, fashionable, and smart sports bras were displayed on the screen in succession, as presented in Figure 1 below. To avoid the influence of their sequential order, stimulating pictures were presented in alternate orders of 123, 231, and 312. Provided that stimulating pictures appeared as programmed on the screen in front of the participants, other variables of the laboratory environment were under strict control, including light, the distance from a participant to the screen, and a quiet laboratory environment. After that, both eye tracker and multi-channel physiological recorder were utilized to collect physiological data from these participants stimulated by product pictures (see Figure 2). Furthermore, the hybrid macro and micro method was employed to analyze their physiological data, investigate consumers' emotional experience when facing these product pictures, and explore correlations between their physiological signals and emotional experience. Therefore, data support can be provided for product design and sales strategies.



FIGURE 1. Experimental materials.

Based on screening through questionnaires, 58 participants were recruited, including 28 males and 30 females with an average age of 24.4. Those participants should not be short-sighted or with myopia degrees below 300°. Before the experiment, all participants were in good condition and informed of basic knowledge about the eye tracker and the multi-channel physiological recorder, and the fundamental procedures of the entire experiment. In addition, they also learned about the fact that this experiment does not harm human bodies and they all signed the corresponding informed consent. Moreover, the experiment lasted for about 25 minutes, and each participant would be awarded RMB 50 as remuneration after the experiment.

Totally, 62 physiological signals about eye movement and multiple channels were collected, including the pupil change rate, the visual retention time, mean HR, HRV, and skin conductance levels. By adding data obtained by multiple little experiments, 2,360 samples were achieved. With the specialized instrument adopted, all data were exported to be structured. After data pre-processing, those samples served as the raw data available for macro affective computing and physiological experiment microanalyses.



FIGURE 2. Data records during the experiment.

III. DATA MACROANALYSIS

Macro affective computing has three procedures of data pre-processing, computing model building, and prediction evaluation. In terms of data pre-processing, feature dimensionality reduction, Box-Cox transformation, principal component analysis (PCA), and normalization were performed. Regarding machine learning, a computing model should be established for physiological data. In this paper, a Stacking ensemble learning model was built with MeanHR relating to affective valence as the dependent variable and other physiological data as the independent variable. In the process of evaluation, Mean Absolute Error (MAE), Mean Square Error (MSE) and R^2 were used as evaluation indicators.

A. DATA PRE-PROCESSING

Data pre-processing consists of several main steps of missing value processing, feature dimensionality reduction, normalization, normal distribution transform, and multicollinearity removal. During missing value processing, bad samples and some other samples containing many missing values are deleted, after which, the dimensionality of the effective dataset stands at (2,360, 60), i.e., 2,360 samples and 62 physiological signal features.

1) FEATURE DIMENSIONALITY REDUCTION

If all features of physiological signals are used as the training set of the proposed computing model, the corresponding training would take a quite long time and certain problems such as overfitting can be also incurred as the number of their features is rather high. In general cases, there are many features insignificantly correlated to target variables. Therefore, a correlation coefficient method was utilized in this paper to perform dimensionality reduction for data.

First, distribution and probability plots of all variables were viewed before the application of the correlation coefficient

method. As there are numerous features, only distribution and probability plots of Feature v0 (i.e., Expansion Rate) were displayed in this section. As shown in Figure 3(a), the blue curve represents the true data, while the black line is a normal distribution curve generated after data fitting. Clearly, the blue line does not coincide with the black line, indicating that the data do not conform to normal distribution. In Figure 3(b), the x-axis and y-axis respectively stand for theoretical quantiles and ordered values. It can be observed that data dots are deviated from the straight line in red, reflecting that these data are in non-conformity with normal distribution. Regarding other features, similar effects are observed. Specific to data in non-conformity with normal distribution, they were figured out by the Spearman Correlation Coefficient (SCC) method, as expressed in Eq. (1) below:

$$\rho = 1 - \frac{6 \sum_{i=1}^n (d_i)^2}{n(n^2-1)} \quad (1)$$

where, $d_i = x_i - y_i$, x and y are values of two variables, and n refers to the number of samples. Values assigned to ρ lie in a range of (-1, 1). If the correlation coefficient is 1, the above two variables are in a perfect positive correlation; if it is -1, this signifies that a perfect negative correlation is formed between the above two variables; and if it is 0, the above two variables are uncorrelated.

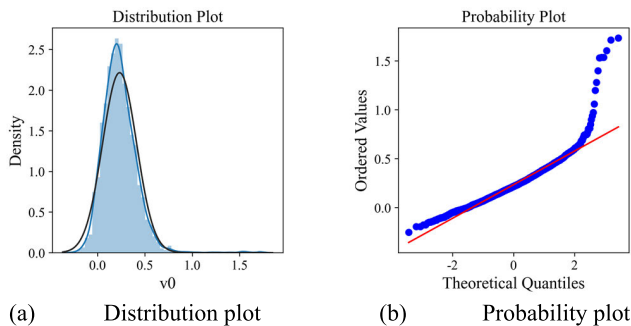


FIGURE 3. Distribution and probability plots of Feature v0.

Correlation coefficients of 61 physiological signal features and the target variable MeanHR were calculated, and relevant results are listed in Figure 4. Among the top 10 features most relevant to the target variable, only seven of them produce correlation coefficients with absolute values above 0.1. Regarding the remaining features whose absolute values of their correlation coefficients with the target variable are smaller than 0.1, their contributions to the computing model are rather insignificant, and they may even place a negative influence on the performance of this model. As for specific correlation coefficients of such seven physiological signal features and the target variable, please refer to Table 1. More particularly, Root Mean Square of Successive Differences (RMSSD), as an indicator of HRV, primarily reveals activity of parasympathetic nerves and forms a negative correlation to SDDSD, and is calculated to be -0.57.

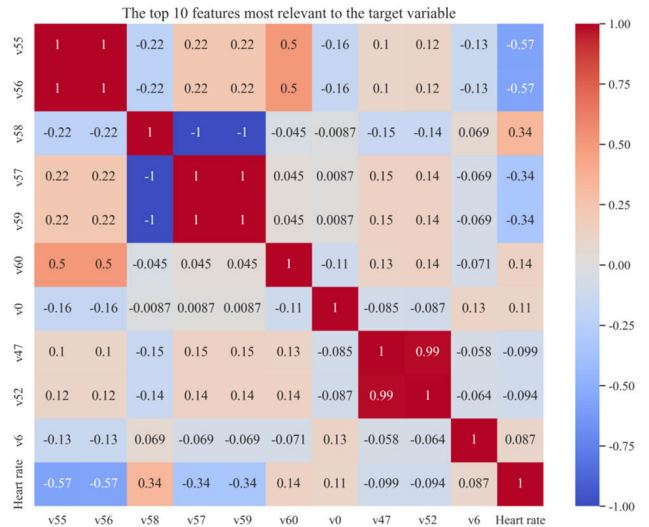


FIGURE 4. The ten features most relevant to the target variable.

TABLE 1. Features relevant to MeanHR.

Feature indexing	Feature name	Correlation coefficient
v0	Expansion Rate	0.11
v55	RMSSD	-0.57
v56	SDDSD	-0.57
v57	Sympathetic	-0.34
v58	Vagal	0.34
v59	Sympathetic-Vagal balance	-0.34
v60	P-P	0.14

Statistically descriptive information of the data after dimensionality reduction has been listed in Table 2. It presents specific information of the involved physiological signal features, such as the total sample count, the mean value, the standard deviation, minimum and maximum values, and the quantiles of these data.

2) NORMAL DISTRIBUTION TRANSFORMATION

Skewed distribution of data may lead to predictor performance degradation; therefore, Box-Cox transformation is conducted for these data as a common data transformation technique in statistical modeling. This aims to make the data closer to normal distribution, and, to some extent, reduce unobservable errors and improve model accuracy. Moreover, Box-Cox transformation can be expressed in the following equations:

$$y^{(\lambda)} = \frac{x^\lambda - 1}{\lambda} (\lambda \neq 0) \quad (2)$$

$$y^{(\lambda)} = \log(x) (\lambda = 0) \quad (3)$$

where, x refers to raw data, $y^{(\lambda)}$ to data after transformation, and λ to Box-Cox transformation parameters. Taking Feature v0 as an example, plots of distribution and probability after/before transformation were presented in Figure 5.

TABLE 2. Data description after feature dimensionality reduction.

Feature indexing	Count	Mean	Std	Min	25%	50%	75%	Max
v0	2360	0.23	0.18	-0.25	0.12	0.22	0.33	1.73
v55	2360	52.17	197.82	4.81	19.87	28.86	45.83	4233.45
v56	2360	51.75	194.57	4.62	19.78	28.64	44.93	4114.38
v57	2360	0.26	0.02	0.08	0.26	0.27	0.28	0.29
v58	2360	0.74	0.02	0.71	0.72	0.73	0.74	0.92
v59	2360	0.36	0.04	0.09	0.35	0.37	0.38	0.41
v60	2360	13.24	9.90	3.02	7.75	11.53	16.13	119.82
MeanHR	2360	81.39	10.76	55.97	72.90	80.38	90.60	109.38

TABLE 3. Data description after the Box-Cox transformation.

Feature Index	Count	Mean	Std	Min	25%	50%	75%	Max
v0	2360	0.31	0.07	0.00	0.26	0.31	0.35	0.60
v55	2360	2.66	0.57	0.00	2.36	2.67	3.01	5.27
v56	2360	2.63	0.55	0.00	2.34	2.64	2.96	5.11
v57	2360	28.99	12.72	0.00	20.08	30.67	38.26	61.06
v58	2360	0.015	0.006	0.00	0.011	0.014	0.019	0.028
v59	2360	14.26	6.21	0.00	9.88	15.01	18.76	30.33
v60	2360	2.17	0.63	0.00	1.73	2.22	2.61	4.65

As can be observed from this figure, real data in v0 transformation plots after transformation are more approximate to the normal distribution curve, and data dots in the probability plot are more approximate to the straight line. As for other features, similar results are observed. In addition, Table 3 shows the results of the normal distribution transformation of seven physiological signals.

3) REMOVAL OF MULTICOLLINEARITY

The correlation coefficients between variables are inherent to the nature of the data itself and relate to the data itself, independent of the data pre-processing method. From Figure 4, it can be seen that the correlation coefficients between individual features are large, for example, the correlation between v55 and v56 is 1 and the correlation between v57 and v58 is -1. Such features can suffer from multicollinearity problems, which can negatively affect the interpretive, stability and predictive performance of the predictor. This problem can be solved by PCA, a data dimensionality reduction technique used to map high-dimensional data into a low-dimensional space, and which retains the main information of the original data, resulting in a linear combination of the original feature vectors. the specific steps of the PCA process are as follows:

Step1, the normalization process, as shown in equation (4),

$$X' = \frac{X - \mu}{\sigma} \tag{4}$$

where X' is the normalized dataset, X is the original dataset, μ is the mean of each feature and σ is the standard deviation of each feature.

Step2, the covariance matrix is calculated, as shown in equation (5),

$$C = \frac{1}{n - 1} \sum_{i=1}^n (X_i - \bar{X})(X_i - \bar{X})^T \tag{5}$$

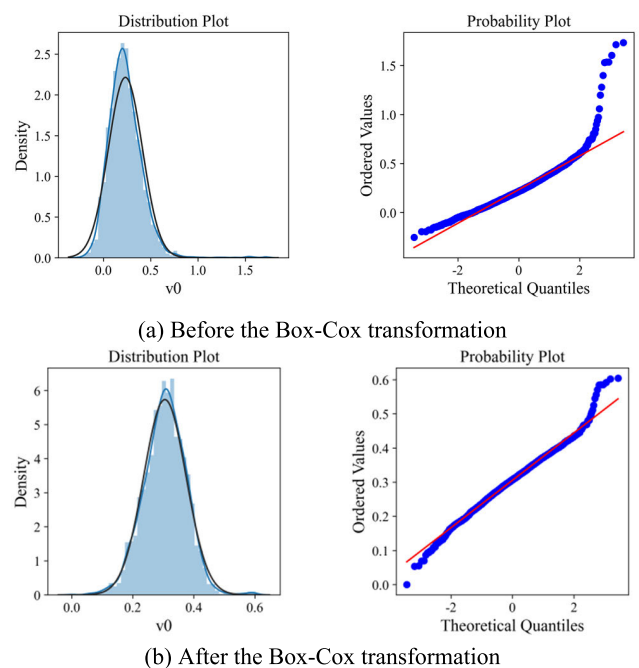


FIGURE 5. Distribution and probability charts.

where C is the covariance matrix, n is the number of samples, X_i is the i -th sample and \bar{X} is the sample mean.

Step3, the eigenvalue decomposition, $Cv = \lambda v$, where v is the eigenvector and λ is the eigenvalue.

Step4, the projection matrix, $W = [v_1 v_2 \dots v_k]$, is calculated by sorting the feature vectors according to their corresponding eigenvalues from largest to smallest, and retaining their four largest features.

Step5, project onto the new basis vector, $X_{new} = XW_k$, where X_{new} is the reduced dimensional data, X is the original

TABLE 4. PCA-processed data descriptions.

New Feature Index	Count	Mean	Std	Min	25%	50%	75%	Max
v0	2360	0.00	14.16	-32.33	-9.93	1.83	10.23	35.88
v1	2360	-0.00	0.88	-3.48	-0.50	-0.05	0.47	3.67
v2	2360	0.00	0.48	-1.61	-0.32	-0.01	0.31	2.69
v3	2360	-0.00	0.07	-0.31	-0.04	0.002	0.05	0.32

TABLE 5. Description of the normalized data.

New Feature Index	Count	Mean	Std	Min	25%	50%	75%	Max
v0	2360	0.47	0.21	0.00	0.33	0.50	0.63	1.00
v1	2360	0.49	0.12	0.00	0.42	0.48	0.55	1.00
v2	2360	0.38	0.11	0.00	0.30	0.37	0.45	1.00
v3	2360	0.49	0.11	0.00	0.42	0.49	0.56	1.00

dataset and W_k is a matrix consisting of the first k ($k=4$) feature vectors.

The four new features obtained by PCA are no longer the original physiological signal features, but it retains important information from the original data while reducing the dimensionality and number of features, Table 4 shows the data descriptions of the four new features obtained by PCA.

4) DIMENSIONLESS PROCESSING

From Table 4, it can be seen that the four new features have different dimensions and value ranges, which may lead to over or under weighting of certain features, thus affecting the training effect and generalization ability of the predictor, in order to eliminate the effect of different dimensions, the data needs to be normalized. Min-Max normalization and Z-score normalization are commonly used data normalization methods. In this study, the Min-Max normalization method was used. Due to the large differences in amplitude and scale between different physiological signal data, if Z-score normalization is used, the scale differences between different signals will be adjusted to the same scale (The mean is 0 and the standard deviation is 1), resulting in information loss, whereas Min-Max normalization can retain the scale information of the original data, thus better mining the relationship between physiological signals and satisfying this study's requirements of the computational model, as in equation (6).

$$x' = \frac{x - \text{Min}}{\text{Max} - \text{Min}} \tag{6}$$

where x is the original data, Min is the minimum value of the data and Max is the maximum value of the data. The normalized data are shown in Table 5.

Figure 6 demonstrates the correlation heat map for the four new features and it can be seen that the correlation between the features is reduced, which effectively avoids the effect of multicollinearity. Figure 7 demonstrates the correlation significance level test for the four new features, as the

p-values between the features and the target variables are all less than 0.05, the overall data correlation is significant and the results are reliable. It can also be seen that some p-values are larger than 0.05 between individual features, while potentially troubling to the interpretation of the model, do not necessarily have a negative impact on the predictive performance of the model, and that the significance level is primarily used in regression models to determine significant correlations between features and target variables.

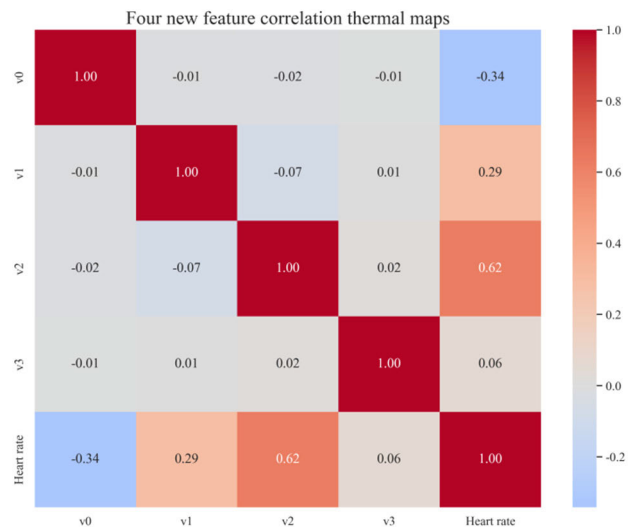


FIGURE 6. Heat map of correlations for new features.

5) DATA SET SLICING

In order to improve the generalization performance of the predictor, the above pre-processed dataset was sliced, where 80% was used to calculate the training set of the model, viz. the dimension of the training set was (1888, 5), and 20% of the data was used as the test set, viz. the dimension of the

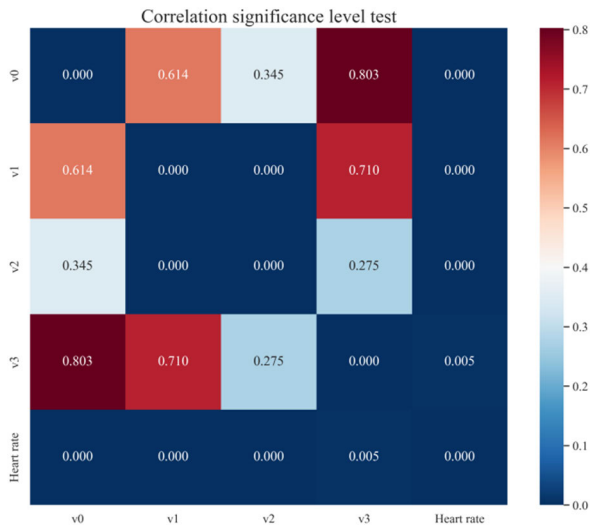


FIGURE 7. Significance level test of correlations for new features.

test set was (472, 5). Using Kernel Density Estimation (KDE) distribution plots to view the cut scores of the four features and target variables, as shown in Figures 8 and 9, it can be seen that the training and test set distributions are generally consistent and can be fed into the computational model for prediction and evaluation.

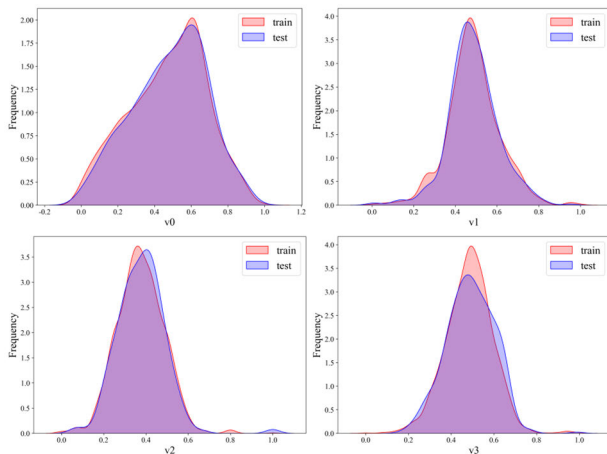


FIGURE 8. KDE distribution of the four features.

B. MACHINE LEARNING MODELS

The emotional valence MeanHR and other physiological signal features were respectively used as dependent and independent variables to build a computing model based on physiological signal features. Under circumstances of numerous physiological signal features, small sample size, and the unclarified relationship between dependent and independent variables, no satisfactory results can be achieved by a deep learning model only. In this case, various deep learning models were tested, and their prediction accuracy was worked out to be around 60%.

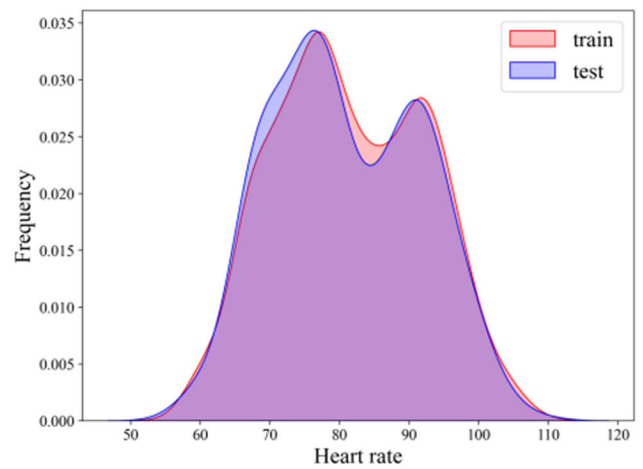


FIGURE 9. KDE distribution of the target variables.

Considering that the dependent variable remains unclear, the stacking ensemble learning model was adopted in this study. Stacking is a second-level learning algorithm. Multiple basic regression models are first used to turn prediction results of the raw data set into new features, and the target variable of such new features is still that of the raw data set. Then, a meta-regression model is trained to perform final prediction, and the corresponding technical route is shown in Figure 10. Basic regression models integrated in this model include Random Forest (RF), Gradient Boosting Decision Tree (GBDT), and Extreme Gradient Boosting (XGB), and also integrate a deep learning model Multi-Scale Convolutional Neural Networks (Multi-Scale CNN).

K-fold cross-validation and Bayesian hyperparameter tuning were utilized in this paper to adjust and optimize model parameters. According to K-fold cross-validation, a dataset is divided into K subsets. While (K-1) subsets serve as a training set, and the other subset as the validation set. Through K repetitions, K estimated values of model performance can be acquired and then averaged. The mean value of these estimated values is used as the model performance indicator. In this way, not only can model overfitting or underfitting be avoided, but model performance can be more accurately estimated. To shorten the computing time, K was set at 5, that is K=5. Bayesian hyperparameter tuning plays a role of searching the parameter space and identifying an optimal combination of hyperparameters. Through prior and posterior distributions, optimal parameter values generating better model performance can be confirmed so as to more efficiently search the parameter space, avoid defects of exhaustive search, and spare time spent on and efforts put in parameter adjustment.

1) DEEP LEARNING MODEL MULTI-SCALE CNN

Multi-Scale CNN is a variant and expansion of convolutional neural network (CNN). Through multi-scale convolutional feature extraction, feature down-sampling,

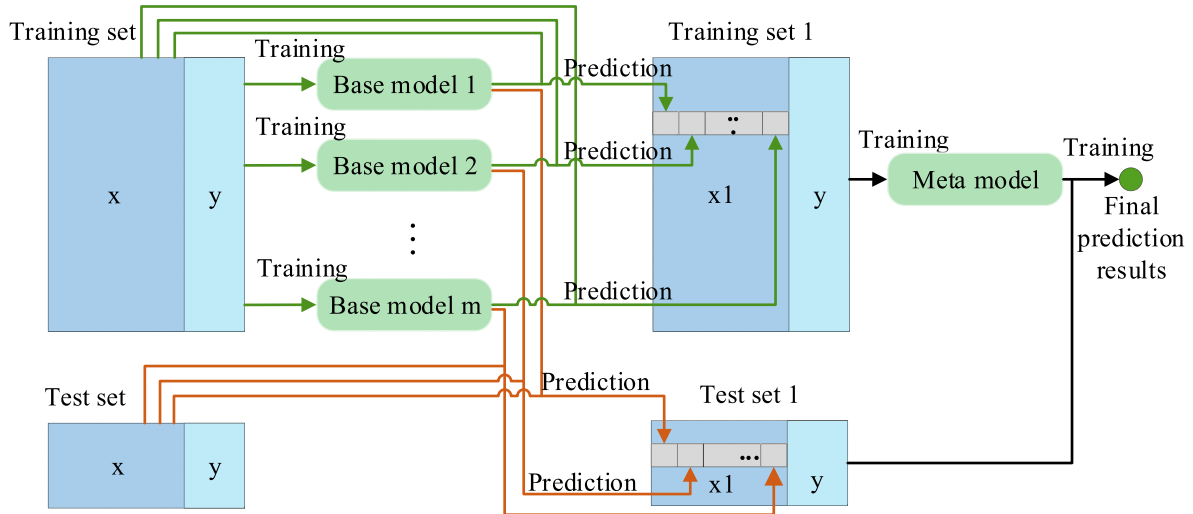


FIGURE 10. Stacking ensemble learning model for physiological signal data.

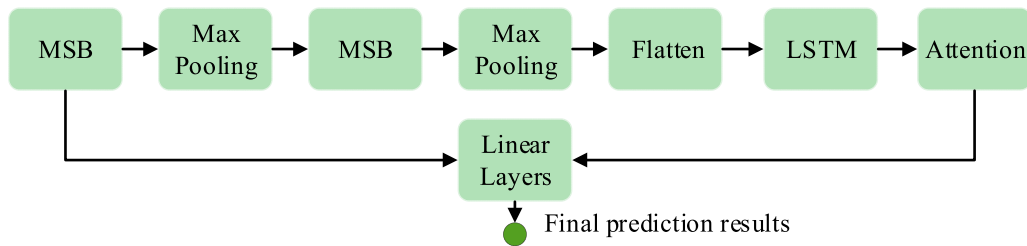


FIGURE 11. Multi-Scale CNN model structure.

sequence modeling, and attentional weighting, multi-scale and sequence information of the input data was combined to generate an integrated feature representation, which is followed by regression. The proposed Multi-Scale CNN in this paper has six steps. (1) A multi-scale convolution block (MSB) containing a single-dimensional convolutional layer, a ReLU activation layer, and a batch normalization layer was developed. By stacking multiple MSBs, convolutional operation is conducted in a condition of different convolution kernel sizes to acquire a multi-scale feature representation of the input data. (2) A maximum pooling layer is provided behind each MSB to perform down-sampling and reduce feature dimensionality. To prevent overfitting, a dropout layer is also mounted, so that some neurons can be randomly outputted to 0. In this way, dependency among neurons is lowered. (3) Multi-scale features of two MSBs are combined and outputted to perform one-dimensional vector flattening, thus facilitating full connection of layers. (4) The long short-term memory (LSTM) layer was adopted to carry out sequence modeling of input. It can effectively process sequential data and extract feature representation with memory capacity. (5) An attentional mechanism layer is also mounted to fulfill the weighting of information in different positions of the sequence. (6) Attentional weighting results are connected to the output of the first MSB, which is followed by input of

full connection and ReLU activation layers, and output of results at last. Moreover, the structure of this Multi-Scale CNN model is depicted in Figure 11.

2) GBDT AND XGB

GBDT and XGB are two well-known representatives of the Boosting ensemble learning method. GBDT is a decision tree based ensemble learning algorithm. It improves model performance by training multiple decision trees in series, and each tree is trained depending on the residual errors of all previous trees. Here, a residual error refers to a difference between the predicted value of a sample in the current model and its true value, enabling the model to approach the actual output value step by step. GBDT regression model can be expressed in the following Eq. (7):

$$\hat{y}_i = \sum_{k=1}^K \gamma_k f_k(x_k) \quad (7)$$

where, \hat{y}_i is an integrating model formed by regression trees. K stands for the number of regression trees, and γ_k to the weight of the k^{th} regression tree. The predicted output of each regression tree is denoted by $f_k(x_k)$. In GBDT, each iteration is aimed at lowering residual errors of the model. Then, during the m^{th} iteration, a residual error requiring fitting is:

$$r_{im} = y_i - \hat{y}_{i,m-1} \quad (8)$$

where, $\hat{y}_{i,m-1}$ represents the predicted values of the previous (m-1) iterations with the aim to make $f_m(x_i)$ better fitting with the residual error r_{im} by fitting a regression tree f_m . It is assumed that the preceding (m-1) trees have been trained, $\hat{y}_{i,m-1}$ is used as the input to perform r_{im} fitting, thus acquiring a result of $\hat{y}_{i,m} = \hat{y}_{i,m-1}$, in which, $\hat{y}_{i,m}$ is the output of m^{th} tree. Moreover, the minimum loss function is:

$$L^{(m)} = \sum_{i=1}^n (y_i - \hat{y}_{i,m-1} - f_m(x_i))^2 \quad (9)$$

Considering that f_m is a regression tree, it is built through CART in line with the regression model. Concretely, the mean value of the target variable is worked out at each leaf node, and then used as the output value of this node. In the process of building this decision tree, a node-splitting approach of the minimum loss function was selected to constantly and iteratively construct a regression tree. At last, the m^{th} tree was obtained.

XGB is evolved from GBDT by introducing normalization, feature weights and other parameters, so as to boost the generalization ability and speed of the model. Loss function of XGB is comprised by two parts. One is the loss function of GBDT, and the other is a normalization term. It can be written into the following formula:

$$\mathcal{L}(\theta) = \sum_{i=1}^n L^{(i)} + \sum_{k=1}^K \Omega(f_k) \quad (10)$$

where, $L^{(i)}$ stands for the loss function of GBDT, f_k for the k^{th} tress, and Ω for the normalization term used to control model complexity and avoid overfitting. Additionally, a normalization term is also introduced on the basis of GBDT in a computational formula expressing weights of leaf nodes as far as XGB is concerned, so as to control model complexity, which results in the following equation:

$$W_j^{(t)} = - \frac{\sum_{i \in I_j^{(t)}} g_i}{\sum_{i \in I_j^{(t)}} h_i + \lambda} \quad (11)$$

where, $W_j^{(t)}$ represents the weight of the j^{th} leaf node during t^{th} iteration; $I_j^{(t)}$ is a sample set falling into the scope of the j^{th} leaf node during t^{th} iteration; and g_i and h_i respectively refer to the gradient and second-order derivative of sample i . λ is the coefficient of the normalization term.

C. PREDICTION AND EVALUATION

Based on the above Stacking ensemble learning model constructed, a predictor was established for the physiological signal MeanHR. Subsequently, 1,888 samples were trained, and the remaining 472 samples were tested to evaluate model performance.

1) EVALUATION INDICATORS

Three evaluation indicators of MAE, MSE and R^2 were used for this study. First, MAE measures the mean absolute error between predicted and true values. The smaller MAE is, the smaller the difference between predicted and true values will

be, indicating that the model is more accurate in prediction, as expressed in Eq. (12):

$$MAE = \frac{1}{n} \sum_{i=1}^n |f_i - y_i| \quad (12)$$

where, n refers to the number of samples, f_i to true values, and y_i to predicted values. Second, MSE is the expected value for a square of the difference between predicted and true values. The lower MSE is, the smaller such a difference will be, indicating higher prediction accuracy of the model. It can be expressed in Eq. (13) below:

$$MSE = \frac{1}{n} \sum_{i=1}^n (f_i - y_i)^2 \quad (13)$$

where, n, f_i and y_i respectively stand for the number of samples, the predicted value, and the true value. Third, R^2 , also known as the determination coefficient, reflects to what extent the regression model interprets changes of the dependent variable, or observed value fitting degrees of the model. It is believed to be a golden standard of regression model judgment, and it ranges from 0 to 1. The closer it is to 1, the better the capability of this model to interpret the target variable will be, as shown in Eq. (14) below:

$$R^2 = 1 - \frac{\sum_{i=0}^n (f_i - y_i)^2}{\sum_{i=0}^n (f_i - \bar{y})^2} \quad (14)$$

where, n is the number of samples, and f_i , y_i and \bar{y} are true values, predicted values, and the mean value, respectively.

2) RESULTS OF THREE FUNDAMENTAL PREDICTORS

RF, GBDT, and XGB predictors were used for the experiment to predict values of MeanHR, as shown in Figure 12. After such tree predictors were adjusted by K-fold cross-validation and Bayesian hyperparameter tuning, the curve of predicted value basically coincides with that of true values, indicating that the predicted value of MeanHR is basically consistent with its true value.

MeanHR prediction results by the above three predictors are shown in Table 6. Respectively, MAEs of MeanHRs predicted by RF, GBDT, and XGB are worked out to be 1.871, 1.040, and 1.260, MSEs to be respectively 8.299, 5.643 and 6.137, and R^2 to be 0.926, 0.950, and 0.946. According to such experimental outcomes, predictors RF, GBDT, and XGB are proven to accurately predict MeanHR. Therefore, these predictors are believed to accurately predict MeanHR values according to physiological signal features, which verifies the feasibility and validity of the proposed data strategy and model design method.

3) PREDICTION RESULTS OF VOTING, BAGGING AND STACKING ENSEMBLE LEARNING PREDICTORS

Three well-trained predictors described in Table 6 and the Multi-Scale CNN were used as the base model to design the following three ensemble learning models of Voting, Bagging, and Stacking in pursuit of higher accuracy and more profound computing experiments. MeanHR prediction

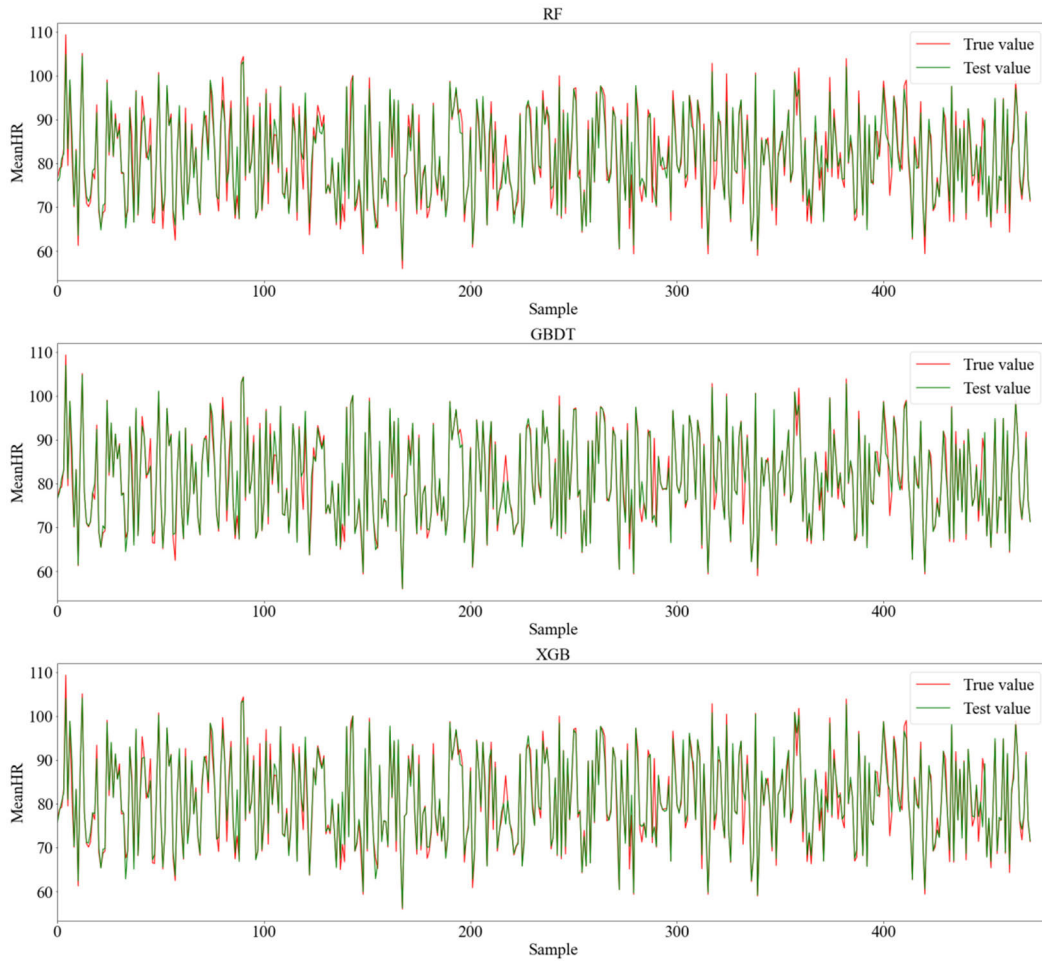


FIGURE 12. MeanHR prediction results of RF, GBDT and XGB predictors.

TABLE 6. MeanHR prediction results.

Predictor	Prediction of MeanHR		
	MAE	MSE	R^2
RF	1.871	8.299	0.926
GBDT	1.040	5.643	0.950
XGB	1.260	6.137	0.946

results by Voting, Bagging and Stacking ensemble learning predictors have been presented in Figure 13. According to this figure, excellent curve fitting is obtained, which verifies the validity of the proposed method again.

Regarding MeanHRs predicted by Voting, Bagging, and Stacking, respectively, their MAEs are calculated to be 1.197, 1.784, and 0.973, MSEs to be 5.943, 8.777, and 5.234, and R^2 to be 0.947, 0.922, and 0.954. Three ensemble learning predictors are thus proven to accurately predict MeanHRs. Combining three base models mentioned above,

the prediction results of six machine learning models are compared, as shown in Figure 14. Clearly, the Stacking ensemble learning predictor constructed based on RF, GBDT, XGB, and Multi-Scale CNN outperforms individual predictors or other ensemble models. For MeanHR prediction by the Stacking predictor, R^2 is 0.004 higher than that obtained by GBDT. RMSSD prediction by the Stacking predictor generates a R^2 value 0.003 greater than that by GBDT. Moreover, the performance of the Stacking predictor in MAE and MSE is the best. In this way, the validity of the Stacking ensemble learning model developed here is highlighted.

IV. DATA MICROANALYSIS

A. DATA MICROANALYSIS

The micro method for physiological data research involves two parts. One is experiment and data collection, a targeted and designed research activity conducted by researchers to solve research assumptions [9]. The other is statistical micro-analysis highly targeted in most cases [41]. However, statistical micro-analysis can consume much manpower and time as

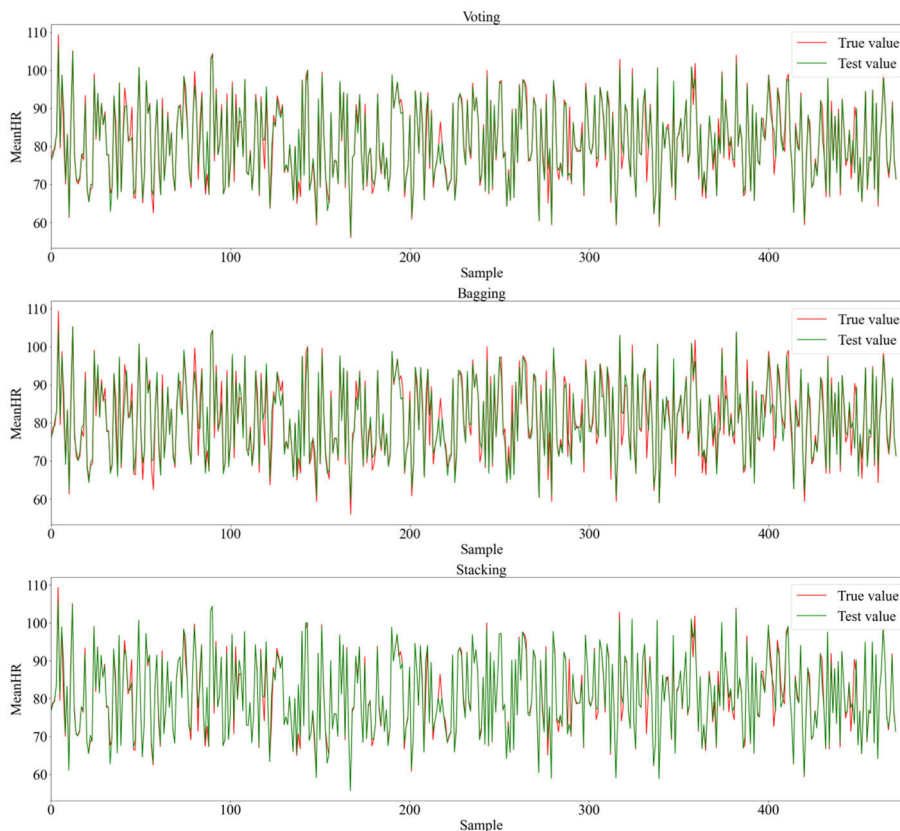


FIGURE 13. MeanHR prediction results of Voting, Bagging and Stacking ensemble learning predictors.

TABLE 7. Prediction results of ensemble learning models.

Predictor	Prediction of heart rate		
	MAE	MSE	R ²
Voting	1.197	5.943	0.947
Bagging	1.784	8.777	0.922
Stacking	0.973	5.234	0.954

it is based on manual operation. In this context, macro computing significantly facilitates the progress of microanalyses.

Macro computing can rapidly identify strongly correlated features, and even find some unexpected valuable information. In this case, the corresponding research of macro computing turns into micro causal relationships, source tracing, and value exploration. For example, both MeanHR and RMSSD are found during macro computing to have a strong correlation with other indicators. According to relevant literature and expertise, MeanHR can explain users' emotional valence and cognitive loads [10], [42]. Considering that stimulus of this experiment is under control, no cognitive load differences exist in this paper. As a result, MeanHR was selected to measure the emotional valence of participants.

Regarding RMSSD, it relates to the activity of parasympathetic nerves and can be used to interpret emotion arousal levels [43].

B. MICROANALYSIS OF CAUSE AND EFFECT

Directed by macro computing results, causality analyses were made on MeanHR and RMSSD. In other words, with the three types of sports bras as the experimental objects, the relationship between these two emotional indicators and consumer behavior and decision-making was explored.

Depending on the analysis of variance with a single-factor, repeated measures, the influence of these sports bras on MeanHRs of research objects was estimated. In the corresponding box plots, no outliers are found in the data (see Figure 15). Through Shapiro-Wilk tests, data in all groups are proved to obey normal distribution ($P > 0.05$). As proved by Mauchly's test of sphericity, dependent variables have equal variance-covariance matrixes, that is $X^2 = 2.079$ and $P = 0.354$. Relevant data are denoted by Mean \pm Standard Deviation ($M \pm SD$). MeanHRs acquired for average, fashionable, and smart sports bras are calculated to be 82.377 ± 9.410 beats per minute, 83.366 ± 9.480 beats per minute, and 83.44 ± 9.451 beats per minute, showing differences with statistical significance where $F(2,94) = 6.375$ and $P = 0.022$. More particularly, the MeanHR of fashionable

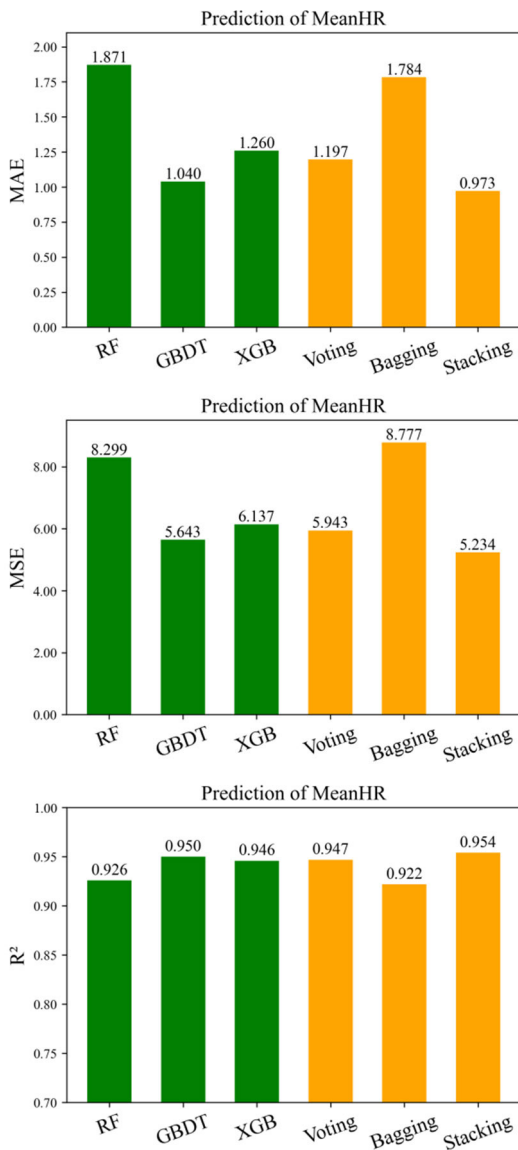


FIGURE 14. Prediction result comparison among six machine learning models.

sports bras is significantly 0.989 higher than that of ordinary sports bras (95% CI: 0.048-1.931), that is $P=0.036$. And compared with sports bras, the MeanHR of smart sports bras is substantially 1.065 greater (95%CI: 0.018-2.112), $P=0.045$.

As data are in non-conformity with normal distribution, a non-parametric test was conducted. Regarding RMSSD, its median was figured out to be 334.16 for average sports bras, 178.563 for fashionable sports bras and 116.142 for smart sports bras. Here, the RMSSD of the above three types of sports bras was compared through the Friedman test. Comparison results indicate that differences in their RMSSDs are statistically significant ($\chi^2 = 7.167, P=0.008$). Post hoc pairwise comparisons during which significance levels were modified by Bonferroni Correction prove that RMSSD differences between fashionable and smart sports bras are of

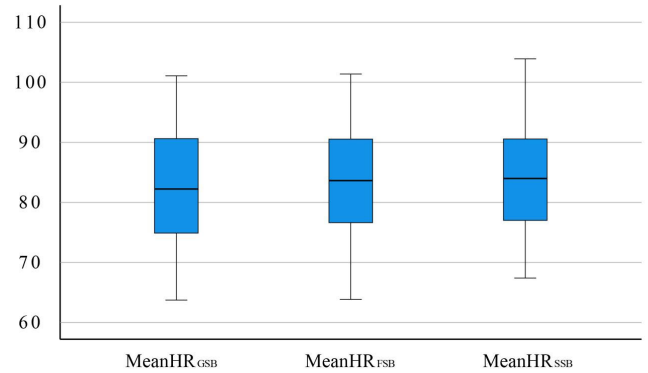


FIGURE 15. Boxplot based verification.

statistical significance (corrected $P=0.009$); however, no statistical significance exists in RMSSD differences between average and fashionable sports bras, where the corrected P value is 0.074, which is nearly significant.

All participants filled in questionnaires after the experiment. 19 of them voted for fashionable sports bras (39.58%), 26 for smart sports bras (54.17%), and only 3 for average sports bras.

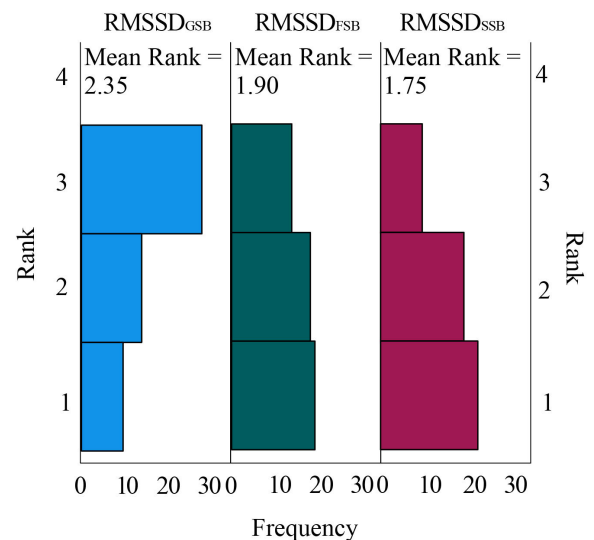


FIGURE 16. Related-samples friedman's two-way analysis of variance by ranks.

V. DISCUSSIONS

A. COMPLEMENTARITY OF MACRO AND MICRO METHODS

This study involves 62 physiological indicators, and researchers are not really familiar with the vast majority of them. Moreover, researchers are inclined to analyze one or several physiological indicators with which they are familiar. This is rather commonly seen in medical science. For example, a doctor may diagnose Obstructive Sleep Apnea Syndrome (OSAS) in line with data collected by a multi-channel

physiological recorder. If it is provided with 64 channels, 64 indicators can be generated; and if it has 256 channels, 256 indicators will be produced. However, diagnosis of OSAS only requires a single indicator of blood oxygen [44], while the remaining unfamiliar indicators are like a blind spot among most doctors, but often imply some important information about OSAS or other associated diseases [45].

For problems collected by an advanced device that cannot be interpreted by researchers, big data and machine learning are considered effective technical routes for the settlement of such problems. In addition to rapidly analyzing all indicators [23], they can rank indicators in descending order according to their correlations with the target variable, as shown in Figure 4. The key to this procedure is to select appropriate data and computing models. Not all data can be used to generate an effective computing model through training. In fact, most data cannot satisfy the requirements of learning models [46]. Additionally, various deep learning models were utilized in the early phases of this study, but no ideal effects were generated. Later, we considered that the physiological signals collected were characterized by a large number of features, small sample size, and comparatively discrete data, so the Stacking ensemble learning model was selected, producing rather good prediction outcomes. Therefore, an ensemble learning model is believed to be more suitable for emotional physiological data similar to those of this study. Big data and machine learning are still able to produce better effects on the premise of unclarified target variables (i.e., the golden standard of disease diagnosis not identified). Without a doubt, they are probably golden standards for rapid diagnosis [28].

Comparatively, macroanalysis has the potential to rapidly identify key indicators. In this study, big data analyses selected can rapidly identify MeanHR and RMSSD as two indicators strongly correlated to other targets. Then, micro quantitative research was conducted to infer emotional indicators of average, fashionable, and smart sports bras, and their associations with consumer behavior. In addition, a micro quantitative study can obtain deep causality by analyzing implicit cognition, explicit behavior, and their relationship.

Furthermore, emotion research involves multiple aspects of various disciplines, and selects different emotional physiological indicators for diverse purposes. Macro affective computing not only provides fundamental breadth analyses in various disciplines, but also provides data support for investigating emotional causality, exploring relevant values and tracing the sources. For instance, HR increase and decrease are more frequently applied as an indicator reflecting functions of ANS. As for the fact of whether they truly reveal the activity of sympathetic nerves and vagus, it remains in dispute [18]. The study by [47] showed that the physiological significance of HR is dramatically affected by time and wavelet scales selected for the computing model investigated. To be concrete, HR increase and decrease both merely depend on vagus activity at a regular scale ($T=1$; $s=2$). At a larger scale of ($T=3$; $s=5$), they form a positive correlation with sympathetic nerve activity, but a negative correlation

with vagus activity. Clearly, macro computing can provide a framework for guiding micro quantitative analyses, set a boundary for micro quantitative analyses, and also prove the role of HR increase and decrease of interpreting ANS activity.

B. VALUES OF EMOTIONAL PHYSIOLOGICAL DATA AND VALUE EXPLORATION

In recent years, objective data acquired from human bodies based on brain and physiological mechanisms are utilized to interpret and investigate behavior and decision-making, which gradually becomes a heatedly discussed topic. As micro emotional physiological signal data can reflect the real human emotions, they are used to interpret human beings' behavior and decision-making [48], and they are rather popular in psychology, education and management science.

In previous studies, MeanHR is a result regulated by interactions of sympathetic and parasympathetic nerves, and cannot directly reflect the activity of a certain nervous system. Now, there are still disputes about the influence of sympathetic and parasympathetic nerves on HRs, and their impacts on HRs are considered different. Some research reported that negative emotions may lead to HR decrease, while others may suggest the opposite conclusion, [49]. Therefore, research on HRs needs to combine other methods in most cases. In terms of RMSSD, as an HRV indicator, it is worked out by extracting the square root from an average value of a square of the difference in two adjacent RRs (interval of two heart beats), and used to evaluate temporal variations of HRs. Specifically, RMSSD mainly reflects the impacts of parasympathetic nerve activity [43]. Compared with MeanHR, RMSSD represents defined meanings. In Table 1, it can be observed that MeanHR and RMSSD have a negative correlation, in line with the conclusion that RMSSD and Mean HR respectively give expressions to the activity of sympathetic and parasympathetic nerves. Furthermore, such a conclusion is further verified in this study from the perspective of big data, and supported by means of combining questionnaires in other studies [18]. Comparatively, the hybrid macro and micro method proposed here can be more objective and universal.

Based on the above conclusions, MeanHR that embodies sympathetic nerve activity was selected in this paper to interpret emotional valence, and RMSSD that reflects parasympathetic nerve activity to interpret emotion arousal levels. According to micro experimental results, smart sports bras enable MeanHR to be significantly greater by 1.065 than average sports bras do, which shows a statistically significant difference. This indicates that the participants prefer smart sports bras. As far as their emotional valence is concerned, it remains consistent with their selection behavior, signifying that consumers are more inclined to buy smart sports bras rather than the average sports bras on the market. MeanHR generated by participants selecting fashionable sports bras is substantially 0.989 (95%CI: 0.048-1.931; $P=0.036$) higher than that of average sports bras. This proves that consumers prefer fashionable bras over average ones. A comparison

of smart and fashionable sports bras shows no significant differences, which is supported by data collected through a questionnaire survey. Such an outcome is needed by designers and product service providers, as it can provide data support for them to learn about consumers' emotional experience and purchase behavior. Results of RMSSD are similar to those of MeanHR just in reverse. As can be observed from Table 1, MeanHR is negatively correlated to RMSSD. Regardless of macro affective computing or micro quantitative analysis on physiological indicators, their results are highly consistent, and also reflects that emotional valence and emotional arousal level share certain similarities.

VI. CONCLUSION AND FUTURE WORK

At present, the physiological mechanism between sympathetic/parasympathetic nerves and emotions is rarely investigated yet. It is less likely to fill such research gaps by a single macro or micro method. In this scenario, multi-modal and system integration approaches are believed to be the key to this problem [11]. The main contributions of this paper can be described from the following two aspects. First, data support is provided for consumer behavior and decision-making research based on physiological data of emotions. Second, a method combining macro affective computing and micro quantitative analysis on emotional data is proposed, involving data collection, macro affective computing, and micro causality. The hybrid macro and micro method is highly universal, and as an innovation of multi-modal data and system integration method, it can be applied in various disciplines such as medical science, psychology, and management science. It can also provide designers, product service providers, and other practitioners with tremendously credible data support.

From the perspective of macro data in this paper, MeanHR reflecting emotional valence and RMSSD giving expressions to emotion arousal levels are strongly correlated, and their correlation coefficient is up to -0.57 . Besides, macro computing-based correlation analysis results are proved to be consistent with results of micro quantitative analysis, signifying that objective physiological data are highly credible and potential values of such data can be more profoundly explored in future work. However, this study still has some defects: (1) The quantitative analysis of micro physiological data is not sufficient, and other indicators represented by physiological data may be investigated in the future to explore the potential values of these data and consumer behavior. (2) Significance of eye movement as an indicator is not reflected in this experiment, and its correlation with other targets is generally low, which is inconsistent with the expected result. Subsequently, more in-depth analyses can be made on the relationship between eye movement and other respective indicators of the multi-channel physiological recorder.

REFERENCES

- [1] M. Sykora, S. Elayan, I. R. Hodgkinson, T. W. Jackson, and A. West, "The power of emotions: Leveraging user generated content for customer experience management," *J. Bus. Res.*, vol. 144, pp. 997–1006, May 2022.
- [2] M. Hassenzahl and A. Monk, "The inference of perceived usability from beauty," *Hum.-Comput. Interact.*, vol. 25, no. 3, pp. 235–260, Jul. 2010.
- [3] M. L. Richins, "Measuring emotions in the consumption experience," *J. Consum. Res.*, vol. 24, no. 2, pp. 127–146, Sep. 1997.
- [4] Y. Chen, "Design and simulation of AI remote terminal user identity recognition system based on reinforcement learning," *Int. J. Model., Simul., Sci. Comput.*, vol. 14, no. 1, Feb. 2023, Art. no. 2341005.
- [5] Y. Cai, X. Li, and J. Li, "Emotion recognition using different sensors, emotion models, methods and datasets: A comprehensive review," *Sensors*, vol. 23, no. 5, p. 2455, Feb. 2023.
- [6] E. H. Houssein, A. Hammad, and A. A. Ali, "Human emotion recognition from EEG-based brain-computer interface using machine learning: A comprehensive review," *Neural Comput. Appl.*, vol. 34, no. 15, pp. 12527–12557, Aug. 2022.
- [7] X. Wang, Y. Ren, Z. Luo, W. He, J. Hong, and Y. Huang, "Deep learning-based EEG emotion recognition: Current trends and future perspectives," *Frontiers Psychol.*, vol. 14, Feb. 2023, Art. no. 1126994.
- [8] M. K. Chowdary and D. J. Hemanth, "Human emotion recognition using intelligent approaches: A review," *Intell. Decis. Technol.*, vol. 13, no. 4, pp. 417–433, Feb. 2020.
- [9] X. Mo, E. Sun, and X. Yang, "Consumer visual attention and behaviour of online clothing," *Int. J. Clothing Sci. Technol.*, vol. 33, no. 3, pp. 305–320, Apr. 2021.
- [10] X. Mo, X. Yang, and B. Hu, "The interaction of clothing design factors: How to attract consumers' visual attention and enhance emotional experience," *J. Fashion Marketing Manag., Int. J.*, vol. 27, no. 2, pp. 220–240, Mar. 2023.
- [11] J. Spiesshoefer, B. Regmi, M. M. Ottaviani, F. Kahles, A. Giannoni, C. Borrelli, C. Passino, V. Macefield, and M. Dreher, "Sympathetic and vagal nerve activity in COPD: Pathophysiology, presumed determinants and underappreciated therapeutic potential," *Frontiers Physiol.*, vol. 13, Jun. 2022, Art. no. 919422.
- [12] P. J. Lang, M. M. Bradley, and B. N. Cuthbert, "Emotion, motivation, and anxiety: Brain mechanisms and psychophysiology," *Biol. Psychiatry*, vol. 44, no. 12, pp. 1248–1263, Dec. 1998.
- [13] S. D. Kreibitz, "Autonomic nervous system activity in emotion: A review," *Biol. Psychol.*, vol. 84, no. 3, pp. 394–421, Jul. 2010.
- [14] N. Zhuang, Y. Zeng, K. Yang, C. Zhang, L. Tong, and B. Yan, "Investigating patterns for self-induced emotion recognition from EEG signals," *Sensors*, vol. 18, no. 3, p. 841, Mar. 2018.
- [15] X. Yang, B. Yang, C. Tang, X. Mo, and B. Hu, "Visual attention quality research for social media applications: A case study on photo sharing applications," *Int. J. Hum.-Comput. Interact.*, pp. 1–14, Apr. 2023.
- [16] D. Lyusin and V. Ovsyannikova, "Measuring two aspects of emotion recognition ability: Accuracy vs. sensitivity," *Learn. Individual Differences*, vol. 52, pp. 129–136, Dec. 2016.
- [17] D. Ismael and A. Ploeger, "Development of a sensory method to detect food-elicited emotions using emotion-color association and eye-tracking," *Foods*, vol. 8, no. 6, p. 217, Jun. 2019.
- [18] X. Yang, B. Lai, and C. Tang, "Experiential product promotions on e-Commerce platform: From the perspective of consumer cognition and emotion," *SAGE Open*, vol. 13, no. 1, Jan. 2023, Art. no. 215824402311538.
- [19] E. Bliss-Moreau, L. A. Williams, and A. C. Santistevan, "The immutability of valence and arousal in the foundation of emotion," *Emotion*, vol. 20, no. 6, pp. 993–1004, 2020.
- [20] I. B. Mauss, R. W. Levenson, L. McCarter, F. H. Wilhelm, and J. J. Gross, "The tie that binds? Coherence among emotion experience, behavior, and physiology," *Emotion*, vol. 5, no. 2, pp. 175–190, 2005.
- [21] C. N. DeWall, R. F. Baumeister, D. S. Chester, and B. J. Bushman, "How often does currently felt emotion predict social behavior and judgment? A meta-analytic test of two theories," *Emotion Rev.*, vol. 8, no. 2, pp. 136–143, Apr. 2016.
- [22] L. Netzer, T. Gutentag, M. Y. Kim, N. Solak, and M. Tamir, "Evaluations of emotions: Distinguishing between affective, behavioral and cognitive components," *Personality Individual Differences*, vol. 135, pp. 13–24, Dec. 2018.
- [23] A. Behler, H.-P. Müller, A. C. Ludolph, and J. Kassubek, "Diffusion tensor imaging in amyotrophic lateral sclerosis: Machine learning for biomarker development," *Int. J. Mol. Sci.*, vol. 24, no. 3, p. 1911, Jan. 2023.

- [24] A. Pradhan and S. Srivastava, "Hierarchical extreme puzzle learning machine-based emotion recognition using multimodal physiological signals," *Biomed. Signal Process. Control*, vol. 83, May 2023, Art. no. 104624.
- [25] A. Garg, V. Chaturvedi, A. B. Kaur, V. Varshney, and A. Parashar, "Machine learning model for mapping of music mood and human emotion based on physiological signals," *Multimedia Tools Appl.*, vol. 81, no. 4, pp. 5137–5177, Feb. 2022.
- [26] K. G. M. Quispe, D. M. Utyiama, E. M. Dos Santos, H. A. Oliveira, and E. J. Souto, "Applying self-supervised representation learning for emotion recognition using physiological signals," *Sensors*, vol. 22, no. 23, p. 9102, Nov. 2022.
- [27] Q. Zhang, H. Zhang, K. Zhou, and L. Zhang, "Developing a physiological signal-based, mean threshold and decision-level fusion algorithm (PMD) for emotion recognition," *Tsinghua Sci. Technol.*, vol. 28, no. 4, pp. 673–685, Aug. 2023.
- [28] S. Tufail, H. Riggs, M. Tariq, and A. I. Sarwat, "Advancements and challenges in machine learning: A comprehensive review of models, libraries, applications, and algorithms," *Electronics*, vol. 12, no. 8, p. 1789, Apr. 2023.
- [29] X. Wang, L. Kou, V. Sugumaran, X. Luo, and H. Zhang, "Emotion correlation mining through deep learning models on natural language text," *IEEE Trans. Cybern.*, vol. 51, no. 9, pp. 4400–4413, Sep. 2021.
- [30] X. Wang, Y. Chang, V. Sugumaran, X. Luo, P. Wang, and H. Zhang, "Implicit emotion relationship mining based on optimal and majority synthesis from multimodal data prediction," *IEEE MultimediaMag.*, vol. 28, no. 2, pp. 96–105, Apr. 2021.
- [31] S. Ko, J. Barnes, J. Dong, C. H. Park, A. Howard, and M. Jeon, "The effects of robot voices and appearances on users' emotion recognition and subjective perception," *Int. J. Humanoid Robot.*, vol. 20, no. 1, Feb. 2023, Art. no. 2350001.
- [32] E. Visted, L. Sørensen, B. Osnes, J. L. Svendsen, P.-E. Binder, and E. Schanche, "The association between self-reported difficulties in emotion regulation and heart rate variability: The salient role of not accepting negative emotions," *Frontiers Psychol.*, vol. 8, p. 328, Mar. 2017.
- [33] D. Kukolja, S. Popović, M. Horvat, B. Kovac, and K. Cosić, "Comparative analysis of emotion estimation methods based on physiological measurements for real-time applications," *Int. J. Hum.-Comput. Stud.*, vol. 72, nos. 10–11, pp. 717–727, Oct. 2014.
- [34] C. Qing, R. Qiao, X. Xu, and Y. Cheng, "Interpretable emotion recognition using EEG signals," *IEEE Access*, vol. 7, pp. 94160–94170, 2019.
- [35] C. Gong, F. Lin, X. Zhou, and X. Lü, "Amygdala-inspired affective computing: To realize personalized intracranial emotions with accurately observed external emotions," *China Commun.*, vol. 16, no. 8, pp. 115–129, Aug. 2019.
- [36] J. Kim and E. André, "Emotion recognition based on physiological changes in music listening," *IEEE Trans. Pattern Anal. Mach. Intell.*, vol. 30, no. 12, pp. 2067–2083, Dec. 2008.
- [37] R. Ribon Fletcher, K. Dobson, M. S. Goodwin, H. Eydgahi, O. Wilder-Smith, D. Fernholz, Y. Kuboyama, E. B. Hedman, M.-Z. Poh, and R. W. Picard, "iCalm: Wearable sensor and network architecture for wirelessly communicating and logging autonomic activity," *IEEE Trans. Inf. Technol. Biomed.*, vol. 14, no. 2, pp. 215–223, Mar. 2010.
- [38] C. D. Katsis, N. S. Katertsidis, and D. I. Fotiadis, "An integrated system based on physiological signals for the assessment of affective states in patients with anxiety disorders," *Biomed. Signal Process. Control*, vol. 6, no. 3, pp. 261–268, Jul. 2011.
- [39] S. C. Widen, J. T. Pochedly, and J. A. Russell, "The development of emotion concepts: A story superiority effect in older children and adolescents," *J. Experim. Child Psychol.*, vol. 131, pp. 186–192, Mar. 2015.
- [40] R. Reisenzein, "Cognition and emotion: A plea for theory," *Cognition Emotion*, vol. 33, no. 1, pp. 109–118, Jan. 2019.
- [41] X. Yang, R. Wang, C. Tang, L. Luo, and X. Mo, "Emotional design for smart product-service system: A case study on smart beds," *J. Cleaner Prod.*, vol. 298, May 2021, Art. no. 126823.
- [42] C. E. Bedford, Y. Nakamura, W. R. Marchand, and E. L. Garland, "Heightened autonomic reactivity to negative affective stimuli among active duty soldiers with PTSD and opioid-treated chronic pain," *Psychiatry Res.*, vol. 309, Mar. 2022, Art. no. 114394.
- [43] S. Geurts, M. J. Tilly, B. Arshi, B. H. C. Stricker, J. A. Kors, J. W. Deckers, N. M. S. de Groot, M. A. Ikram, and M. Kavousi, "Heart rate variability and atrial fibrillation in the general population: A longitudinal and Mendelian randomization study," *Clin. Res. Cardiol.*, vol. 112, no. 6, pp. 747–758, Jun. 2023.
- [44] S. Y. C. Liu, M. Abdelwahab, P. Chao, Y. Lee, A. Chen, and C. Kushida, "0732 sonographic phenotyping of the upper airway in OSA using backscattered imaging analyzed by machine-learning," *Sleep*, vol. 45, p. 320, May 2022.
- [45] S. J. Holfinger, M. M. Lyons, B. T. Keenan, D. R. Mazzotti, J. Mindel, G. Maislin, P. A. Cistulli, K. Sutherland, N. McArdle, B. Singh, N.-H. Chen, T. Gislason, T. Penzel, F. Han, Q. Y. Li, R. Schwab, A. I. Pack, and U. J. Magalang, "Diagnostic performance of machine learning-derived OSA prediction tools in large clinical and community-based samples," *Chest*, vol. 161, no. 3, pp. 807–817, Mar. 2022.
- [46] S. D. Latif and A. N. Ahmed, "A review of deep learning and machine learning techniques for hydrological inflow forecasting," *Environ., Develop. Sustainability*, pp. 1–28, Mar. 2023.
- [47] Q. Pan, G. Zhou, R. Wang, G. Cai, J. Yan, L. Fang, and G. Ning, "Do the deceleration/acceleration capacities of heart rate reflect cardiac sympathetic or vagal activity? A model study," *Med. Biol. Eng. Comput.*, vol. 54, no. 12, pp. 1921–1933, Dec. 2016.
- [48] Buy Fogg. (Mar. 4, 2023). *Fogg Behavior Model[EB/OL]*. [Online]. Available: www.behaviormodel.org
- [49] G. J. Norman, G. G. Berntson, and J. T. Cacioppo, "Emotion, somatovisceral afference, and autonomic regulation," *Emotion Rev.*, vol. 6, no. 2, pp. 113–123, Apr. 2014.



MO XIAOHONG was born in Guangdong, China. She is currently pursuing the Ph.D. degree with the School of Art and Design, Guangdong University of Technology. She is also a senior designer with design company. Her research interests include cognitive psychology for design, including consumer behavior analysis and consumer visual attention related to design.



XIE ZHIHAO was born in Guangzhou, in July 1999. He is currently pursuing the master's degree in engineering with the Guangdong Key Laboratory of Computer Integrated Manufacturing of Guangdong Province, Guangdong University of Technology. His research interests include machine learning, data warehousing, and big data platform application development. He has won awards, such as China University Big Data Challenge.



LUH DING-BANG received the Graduate degree from the Illinois Institute of Technology. He was the Dean of the School of Creative Design, Asia University. He is currently a national high-level talent in the field of culture and art in China. He is also the first batch of design doctor in USA. He is also a Distinguished Professor with the School of Art and Design, Guangdong University of Technology. He is also the Chairperson of the Taiwan Design Innovation Management Association and the Chairperson of the International Service Innovation Design Association.

• • •